Fast Simultaneous B_0/B_1 Mapping by Bloch-Siegert Shift with Improved Gradient Scheme and Pulse Design

Qi Duan[1], Peter van Gelderen[1], and Jeff H. Duyn[1]

[1]*Advanced MRI section, LFMI, NINDS, National Institutes of Health, Bethesda, MD, United States*

Introduction

In MRI, spatial variations in the RF transmit field (B_1^+ field) can result in imprecise volume selection, and can affect contrast and sensitivity. B_1 mapping techniques provide a way to quantify this inhomogeneity, and mitigate its effect on image quality [1-4]. Recently, a method based on the Bloch-Siegert (BS) effect [5] has been shown to allow B_1 mapping with relatively little dependence on TR, T_1 relaxation, flip angle, chemical shift, B_0 inhomogeneity, and magnetization transfer. However, the minimum measurement time allowed by the BS method is generally limited by the allowable Specific Absorption Rate (SAR), which may become quite restrictive for human scanning at 7T and above. Based on theoretical analysis of the dependence between mapping sensitivity and SAR levels, we developed an approach to reduce SAR levels and further improving insensitivity to B_0 inhomogeneity compared to the original implementation [5]. The effectiveness of the new scheme is demonstrated in human brain at 7T.

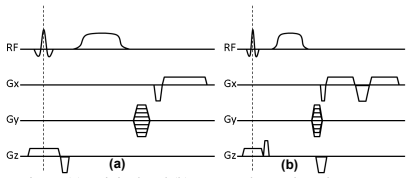

Fig. 1: (a) Original and (b) proposed GRE based BS B_1 mapping sequence diagram

Methods

For a BS pulse with constant frequency offset ω_{RF}, the BS phase shift $\phi_{BS} = \gamma^2/(2\omega_{RF}) \cdot \int_0^T (B_1(t))^2 dt$ [5], from which it can be shown that $SAR \propto 2\phi_{BS}\omega_{RF}/\gamma^2$, i.e. the SAR of the BS pulse is proportional to the ϕ_{BS} for a constant frequency pulse. Since ϕ_{BS} directly determines the signal strength in the final B_1 map, the only way to reduce SAR without affecting mapping sensitivity is to reduce ω_{RF}. In practice, reducing ω_{RF} increases the risk of artifacts that relate to the direct excitation of spins by the BS pulse. To reduce such effect, generally there are three options: (1) the use of gradients to dephase the signal excited by the BS pulse, and (2) optimizing the pulse shape to have minimal energy in the so-called "stop-band" outside a pre-selected frequency band (i.e. "pass-band"), (3) stretching the pulse thereby reducing the bandwidth; the last (trivial) option has not been explored here.

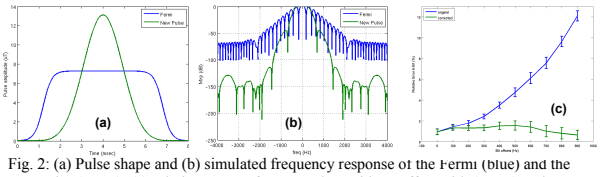

Fig. 2: (a) Pulse shape and (b) simulated frequency response of the Fermi (blue) and the new pulse (green). (c) relative errors of measured B_1 with B_0 offset with (green) and without (blue) simultaneous correction.

Improved Gradient Scheme: The original and improved gradient schemes are shown Fig. 1a and b respectively. Generally, a bipolar crusher pair sandwiches the BS pulse (the first crusher is combined with the slice rephasing gradient). Signal excited by the imaging pulse is properly rephased, while any signal excited by the BS pulse is dephased by the second crusher.

Improved Pulse Shape: The direct excitation effect can be further reduced by improving the stop-band performance of the BS pulse, as demonstrated in [6]. In the pulse optimization for this work, the BS shift is maximized for a fixed peak B_1 value, for each pulse shape generated by the stop-band response minimization using the method proposed in [7]. Detailed design parameters are: the pulse duration 8ms (same as the original Fermi pulse); ω_{RF} is set to ±2kHz, giving four-fold savings in SAR in comparison with the ±8kHz Fermi pulse; passband ripple tolerance is set to a high value (e.g. 50%) to increase flexibility in the pulse shape optimization; bandwidth 1kHz; and maximum stop-band ripple tolerance 1e-4. The shape and simulated frequency response for the final optimized pulse as well as the original Fermi pulse that generates 45° BS phase shift are plotted in Fig. 2a,b.

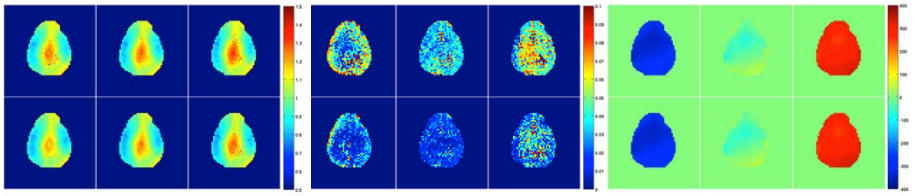

Fig. 3: in vivo results: relative B_1 maps after B_0 correction (left panel, scaled from 50% to 150%), relative error maps (middle panel, scaled from 0% to 10%), and B_0 maps (right panel, scaled from -400Hz to 400Hz). The top row images were acquired with 2kHz 8ms Fermi pulse and the bottom row with the new pulse. The B_0 offset was -300 Hz in left column, 0 Hz in the middle, and +300 Hz in the right column of each panel.

Simultaneous B_0 correction: Reducing ω_{RF} will also increase the sensitivity to B_0 inhomogeneity. For this reason, simultaneous B_0 measurement was added into the sequence (Fig. 1b), and used to correctly calculate B_1 values from the measured BS shifts.

Results

The effectiveness of the proposed sequence was demonstrated both with an oil phantom scan and an IRB approved volunteer study. All experiments were performed on a Siemens Magnetom 7T (Erlangen, Germany) scanner based on an Agilent 7T-830-AS (Oxford, UK) magnet, with a 32-channel head coil (Nova Medical Inc., Wilmington, MA, USA). The phantom data showed that the improved gradient scheme reduces the on-resonance effect of a ±2kHz Fermi pulse 250-fold (or 48dB) for the Fermi pulse. Fig. 2c shows that simultaneous B_0 correction allows accurate B_1 measurements with up to a 1kHz B_0 offsets.

B_0 Offset (Hz)	-300	0	300
Mean Error (Fermi)	4.5%	3.5%	5.1%
Mean Error (New Pulse)	2.4%	1.6%	3.1%

Table 1: Mean relative errors in B_1 map.

Common imaging parameters for in vivo study were: FOV 256mm, imaging matrix 64x64, flip angle 15°, slice thickness 5mm, SAR level 98% of maximum. First, the reference B_1 map was acquired with an ±8kHz Fermi pulse (nominal ϕ_{BS}=30°, TR = 720ms, 10 repetitions, acquisition time (TA) = 15m22s). Then single repetition B_1 maps using the proposed gradient scheme with a ±2kHz Fermi pulse and the new pulse were acquired with B_0 offsets at -300Hz, 0Hz, and 300Hz (nominal ϕ_{BS}=30°, TR=180 ms, TA=23s). Finally, to illustrate the advantage of reducing frequency offset for fast acquisition, angle-to-noise ratio (ANR) maps for the new ±2kHz pulse (nominal ϕ_{BS}=30°) and ±8kHz Fermi pulse (nominal ϕ_{BS}=7.5°) with TR=180ms were calculated from 10 repeated scans (TA=3m50s) by dividing their mean phase shift by their standard deviation (over repetitions).

Fig. 3 shows (a) the relative B_1 maps as well as (b) the relative error maps for both pulses at (c) different B_0 offsets. The mean relative errors are presented in Table 1. The ANR maps are shown in Fig. 4, with average ANR with the ROI as 89.7 and 33.8, respectively. This shows the advantage of reducing SAR via reducing ω_{RF} instead of ϕ_{BS}.

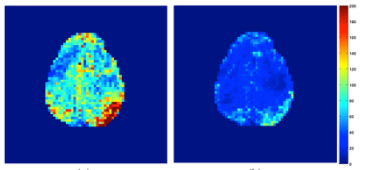

Fig. 4: in vivo results: angle-to-noise ratio maps (scaled from 0 to 200) acquired by (a) 2kHz the new pulse and (b) 8kHz Fermi pulse with 10 repetitions. SAR = 98% and TA = 3m50s.

Conclusions

An optimized shape for the off-resonance pulse used in BS B_1 mapping techniques combined with a modified gradient scheme and simultaneous B_0 mapping allow much reduced frequency offsets to be used. The resulting increase in the BS phase shift leads to improved B_1 accuracy for a given SAR, as demonstrated in both phantom and human studies. Although not investigated in this abstract, by making the pulse longer, the effective bandwidth of the pulse can be further reduced, allowing further reduction of ω_{RF} and thus the SAR and/or further increase of ϕ_{BS} and SNR in the B_1 map. The proposed scheme can be combined with other optimization scheme, e.g. EPI readout, to further reduce the SAR requirement.

References

[1] Sacolick, et al, MRM 2011. [2] Hoult, et al, JMRI 2000, 12(1):46-67. [3] Zhu, et al, MRM 2004; 52(4): 869-77. [4] Katscher, et al, MRM 2003, 49(1):144-50. [5] Sacolick, et al, MRM 2010; 63(5): 1315-22. [6] Khalighi, et al, ISMRM 2011: 4431. [7] Selesnick, et al, IEEE TSP 1996; 44(8): 1879-92.